Ecotoxicology and Environmental Safety 237 (2022) 113512

Contents lists available at ScienceDirect

Ecotoxicology and Environmental Safety

journal homepage: www.elsevier.com/locate/ecoenv

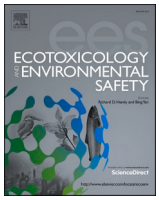

Maternal exposure to ambient $PM_{2.5}$ causes fetal growth restriction *via* the inhibition of spiral artery remodeling in mice

Shimin Tao [a,1], Xuan Zhang [a,1], Fang Tian [a], Bin Pan [b], Renzhen Peng [b], Yuzhu Wang [a], Minjie Xia [a], Mingjun Yang [a], Jingying Hu [a], Haidong Kan [b], Yanyi Xu [b,*], Weihua Li [a,**]

[a] NHC Key Lab of Reproduction Regulation (Shanghai Institute for Biomedical and Pharmaceutical Technologies), School of Pharmacy, Fudan University, Shanghai 200032, China

[b] Department of Environmental Health, School of Public Health, Fudan University, Shanghai 200032, China

ARTICLE INFO

Edited by Dr Fernando Barbosa

Keywords:
Maternal exposure
$PM_{2.5}$
Fetal growth restriction
Spiral artery remodeling
Inflammation

ABSTRACT

Background: Maternal exposure to ambient fine particulate matters ($PM_{2.5}$) is associated with low birth weight (LBW) in offspring, but the underlying biological mechanisms are not yet fully understood. As the bridge that connects mother and fetus, the placenta plays a crucial role in fetal development by providing the fetus with nutrients and oxygen. However, whether $PM_{2.5}$ exposure would impact the placental development and the related mechanisms are unclear.

Results: In the present study, female C57Bl/6j mice were exposed to filtered air (FA) or concentrated ambient $PM_{2.5}$ (CAP) during pregestational and gestational periods, and the fetal development and placental structure were investigated. Our results showed that maternal exposure to CAP induced fetal growth restriction (FGR) and LBW. The placenta from CAP-exposed mice exhibited abnormal development including significant decrease of surface area, smaller junctional zone and impaired spiral artery remodeling. Meanwhile, CAP exposure altered trophoblast lineage differentiation and disrupted the balance between angiogenic and angiostatic factors in placenta. In addition, the inflammatory cytokines levels in lung, placenta and serum were significantly increased after ambient $PM_{2.5}$ exposure.

Conclusion: Our findings indicate that maternal exposure to $PM_{2.5}$ disrupts normal structure and spiral artery remodeling of placenta and further induces FGR and LBW. This effect may be caused by the placental inflammation response subsequent to the pulmonary and systemic inflammation induced by ambient $PM_{2.5}$ exposure.

1. Introduction

It is estimated that over 90% of world's population live in areas where ambient fine particulate matters ($PM_{2.5}$) concentrations are greater than the World Health Organization guideline (annual average of 5 μg/m^3 as updated this year) (Shaddick et al., 2020). A recent study has indicated that air pollution is the fourth-ranking global mortality risk factor for both male and female, and the death globally caused by air pollution (mainly from ambient $PM_{2.5}$ and ozone exposure) is approximately 6.67 million in 2019 representing about 12% of total global mortality (Murray et al., 2020). The public health issues caused by $PM_{2.5}$ have got more and more attentions across the world, especially in China

Abbreviations: $PM_{2.5}$, particulate matter with an aerodynamic diameter ≤ 2.5 μm; CAP, concentrated ambient $PM_{2.5}$; FA, filtered air; GD, gestation day; LBW, low birth weights; FGR, fetal growth restriction; CRL, crown-to-rump length; PAHs, polycyclic aromatic hydrocarbons; VACES, versatile aerosol concentration enrichment system; EDCs, endocrine-disrupting chemicals; PBS, phosphate buffer saline; H&E, hematoxylin and eosin; BAT, brown adipose tissue; VEGF, vascular endothelial growth factor; PLGF, placental growth factor; VSMCs, vascular smooth muscle cells; SpT, spongiotrophoblast; GCs, glycogen trophoblast cells; TGCs, trophoblast giant cells; P-TGCs, parietal TGCs; SpA-TGCs, spiral artery associated TGCs; S-TGCs, maternal sinusoidal TGCs.

* Correspondence to: Department of Environmental Health, School of Public Health, Fudan University, 130 Dong'an Rd, Shanghai 200032, China.

** Correspondence to: NHC Key Lab of Reproduction Regulation (Shanghai Institute for Biomedical and Pharmaceutical Technologies), Fudan University, 2140 Xie Tu Road, Shanghai 200032, China.

E-mail addresses: 18111150003@fudan.edu.cn (S. Tao), xuanzhang@sippr.org.cn (X. Zhang), fannietian@qq.com (F. Tian), 18211020079@fudan.edu.cn (B. Pan), 19211020020@fudan.edu.cn (R. Peng), wangyz1@cansinosph.com (Y. Wang), xiaminjie@sibpt.com (M. Xia), yangmingjun@sibpt.com (M. Yang), hujingying@sibpt.com (J. Hu), kanh@fudan.edu.cn (H. Kan), yanyi_xu@fudan.edu.cn (Y. Xu), weihua.li@sibpt.com (W. Li).

[1] These authors contributed equally to this work.

https://doi.org/10.1016/j.ecoenv.2022.113512
Received 16 November 2021; Received in revised form 30 March 2022; Accepted 8 April 2022
Available online 13 April 2022

and other developing countries (Nel, 2005; Chen et al., 2017). In the past several years, growing number of epidemiological and toxicological studies have found that maternal exposure to $PM_{2.5}$ may influence the normal development of fetus, leading to fetal growth restriction (FGR) and low birth weight (LBW) (Janssen et al., 2017; Liu et al., 2007). Moreover, these adverse birth outcomes may further contribute to the increased risk of health problems such as cognitive disorders, cardiovascular diseases, diabetes and metabolic syndrome at adulthood (Gluckman et al., 2008; Sharma, Farahbakhsh, et al., 2016). However, the underlying molecular mechanisms of abnormal fetal development caused by $PM_{2.5}$ exposure are not yet well understood.

FGR occurs when the fetus fails to achieve its genetic growth potential, and it is a complicated disorder with multiple causes. Studies have found that FGR may originate from maternal or fetal factors such as undernutrition in mother or specific genetic defects in the embryo. Although the precise biological mechanisms of FGR remain unknown, there's evidence that it's strongly associated with the placental dysfunction (Sharma, Shastri, et al., 2016). The placenta is thought to act as a bridge connecting mother and fetus, and play a critical role in regulating nutrient supply to the growing embryo during pregnancy. Hence, adequate placental function is crucial to the fetus growth (Burton et al., 2016). Proper placental development needs coordinated fetal trophoblast invasion and maternal spiral artery remodeling, and disruption of these processes can result in a reduction of blood flow to the placenta and fetus, subsequently leading to FGR (Brosens et al., 2011). Previous studies have suggested that endocrine disrupting chemicals (EDCs) such as bisphenol A and polychlorinated biphenyls may disrupt the spiral artery remodeling process and cause harmful effects to the developing fetus (Muller et al., 2018; Tewari et al., 2009). Considering that $PM_{2.5}$ contains non-negligible amount of EDCs such as heavy metals and Polycyclic Aromatic Hydrocarbons (PAHs), $PM_{2.5}$ may induce FGR *via* the disruption of spiral artery remodeling process.

So far, there are limited studies exploring the association between $PM_{2.5}$ exposure and placental dysfunction. Veras et al. found that maternal $PM_{2.5}$ exposure could cause decrease of fetus weight accompanied by reduced area of maternal blood space and increased fetal capillary surface area in placenta (Veras et al., 2008). A recent study has indicated that gestational exposure to $PM_{2.5}$ resulted in adverse outcomes including FGR and LBW with significant changes in placental weight (Blum et al., 2017). In addition, animal studies found that maternal exposure to $PM_{2.5}$ could impair labyrinthine vascularization, disturb the nutrient transportation, and change the renin-angiotensin system in the placenta (Yue et al., 2019; Zhu et al., 2021; Soto et al., 2017). *In vitro* experiments suggested that $PM_{2.5}$ remarkedly induced cellular toxicity in trophoblast cells, caused hormone dysregulation, oxidative stress, inflammation, endoplasmic reticulum stress and mitochondrial interference (Naav et al., 2020; Familari et al., 2019). In the present study, to understand the underlying toxicological mechanisms of $PM_{2.5}$ induced FGR, we investigated the effects of $PM_{2.5}$ exposure on the processes of trophoblast differentiation and spiral artery remodeling in placenta. Meanwhile, the angiogenesis and inflammation conditions were also assessed.

2. Materials and methods

2.1. Animals

Female C57BL/6J mice of 4-week-old were purchased from the Animal Center of Shanghai Medical School, Fudan University (Shanghai, China) and freely accessed to sterile water and standard food. All the mice were maintained in a climate-controlled room under a relative humidity of 55% ± 10% and a 12 h alternating light/dark at 22 ± 2 °C throughout the study. All procedures and protocols of this study were approved by the Institutional Animal Care and Use Committee (IACUC) at Fudan University, and all the animals were treated humanely and with regard for alleviation of suffering.

2.2. Exposure procedure

After 1 week of acclimation, 5-week-old female mice were exposed to FA (n = 20) or CAP (n = 18) for 13 weeks before copulation. The 18 weeks-old female mice were then mated with normal non-exposed C57Bl/6 J male mice (1 male mating with 2 females). During the mating period, the presence of sperm plug was checked twice a day. Upon the presence of sperm plug, the day was considered as the gestational day (GD) 0.5. Subsequently, the pregnant mice were continuously exposed to FA/CAP until GD16.5 or until natural delivery. The FA/CAP exposure was performed using the versatile aerosol concentration enrichment system (VACES) that was modified for long-term exposures (Ying et al., 2014). The exposure protocol comprised exposures for 8 h per day and 5 days per week (no exposure took place during the weekends). Body weights were evaluated weekly before pregnancy and on GD 0.5, 6.5, 9.5, 12.5, 15.5 and 16.5 during pregnancy. $PM_{2.5}$ samples in the FA and CAP chambers were collected weekly, and the compositions of these $PM_{2.5}$ samples were determined by X-ray fluorescence spectrometry (XFS).

2.3. Tissue collection and fetal examination

After exposure, the pregnant mice from FA (n = 10) or CAP (n = 8) group was euthanized on GD17.5 and their blood was harvested from the orbital venous plexus. The main organs including heart, liver, spleen, lung, kidney, thymus, pancreas, brain, ovary, fallopian tube, uterus, parametrial adipose tissue, subcutaneous adipose tissue, and brown adipose tissue (BAT) were collected and immediately weighed. Then the uterus was carefully opened, the fetuses and placenta of each mouse were excised and weighed, with the crown-to-rump length (CRL) and tail length of each fetus determined using digital calipers. The placentae were photographed and their sizes were measured using Image J Software (Version 1.3, National Institutes of Health). The tail of each mouse was nipped, collected and frozen at − 80 °C for sex determination. Part of the fetus and placenta were fixed in 4% paraformaldehyde and processed for pathologic analysis, and the others were snap-frozen in liquid nitrogen and then stored at − 80 °C for further use. The other pregnant dams (n = 10/group) were permitted to deliver naturally, and the number of alive/dead fetuses were recorded. The body weight, body length and tail length of each alive fetus was also measured at birth.

2.4. Sex determination

Sex determination of the fetus was performed using the isolated tail DNA following the protocol as described by previous study (Blum et al., 2012). PCR was performed using primers for the sex-determining region of chromosome Y (SRY) gene (5′- TTG TCT AGA GAG CAT GGA GGG CCA TGT CAA; 5′-CCA CTC CTC TGT GAC ACT TTA GCC CTC CGA). The reactions were performed for 30 cycles (95 °C for 30 s, 60 °C for 20 s, 72 °C for 1 min). After PCR, products were separated using 1% agarose gels, and sex was determined by visualization of ethidium bromide bands under ultraviolet light illumination.

2.5. Histological analysis of placenta tissues

The placentae were fixed in 4% paraformaldehyde overnight at 4 °C, washed in phosphate buffer saline (PBS), dehydrated in a graded series of ethanol and xylene solutions, embedded in paraffin, cut into 5-μm-thick sections at the mid sagittal plane with a microtome (Leica Microtome RM2235, Leica), and subjected to hematoxylin and eosin (H&E) staining. Histological images were obtained with a slide scanner microscope equipped with a 20x objective (VS120 virtual Slide, Olympus). The areas of the placental cross-section, junctional zone, labyrinth zone and maternal decidua zone were assessed with Image J software. The luminal and total cross-sectional areas of spiral arteries in maternal decidua zone were identified and measured, and the ratio of total vessel

area to luminal area was calculated as an indicator of spiral artery remodeling.

2.6. Immunohistochemical (IHC) staining

The placental sections were processed for immunohistochemical staining using routine procedures. Briefly, the dewaxing placental sections were immersed in diluted citrate buffer (Beyotime, China) for 20 min in a 98 °C water bath for antigen retrieval. To quench the endogenous peroxidase activities, the sections were treated with 3% H_2O_2 in methanol (Beyotime, China) for 15 min at room temperature. After blocked with 10% goat serum for 30 min at room temperature, and incubated with mouse monoclonal α-SMA (1:200 dilution) antibody (Boster, China) overnight at 4 °C, sections were washed with PBS, incubated with HRP anti-mouse secondary antibody (Beyotime, China) at 37 °C for 1 h, and then treated with DAB-HRP chromogenic agent (Beyotime, China) at room temperature for 20 min. For the negative control, normal rabbit IgG (Beyotime, China) instead of the primary antibody was used. Images were obtained on a microscope (Nikon, Japan) using the same light intensity, camera gain and microscope magnification, and analyzed using Image J software. The loss of smooth muscle cells (α-SMA-positive cells) was detected and evaluated by % of circumference as described in previous study (Przybyl et al., 2016).

2.7. Enzyme-linked immunosorbent assay (ELISA)

Placental samples were homogenized in RIPA lysis buffer with protease inhibitor cocktail (Beyotime, China), and the protein concentration of each extraction was determined with a BCA assay kit (Beyotime, China). The vascular endothelial growth factor A (VEGFA), placental growth factor (PLGF) and fms related receptor tyrosine kinase 1 (FLT1) levels were measured using commercially available ELISA kits (Boster, China) according to the manufacturer's instructions.

2.8. Assessment of serum, pulmonary and placental cytokines levels

Levels of TNFα, IL-6, IL-10, IL-12 (p70), MCP1 and IFNγ in serum, lung and placenta tissues were measured using the cytometric bead array (mouse inflammation kit, BD Biosciences, USA) according to the manufacturer's instructions.

2.9. Real-time RT-PCR

RNA was extracted from placental tissues and purified using the TRIzol reagent (Invitrogen, USA). 2 μg of total RNA was reverse transcribed into cDNA using High Capacity cDNA Reverse Transcription Kit (Invitrogen, USA) per manufacturer's instruction. Real-time RT-PCR was performed by Lightcycler 480 using SYBER Green PCR Master Mix (Applied Biosystems, USA). After amplification, a dissociation curve was analyzed to ensure the purity of PCR products. The primers sequences were listed in Table S1. Ct values were obtained through analysis with software provided by the manufacturer, and differences of Ct values between target genes and GAPDH (ΔCt) and $2^{\Delta Ct}$ were then calculated.

2.10. Statistics

All data are expressed as means ± standard errors of the mean (SEMs) unless noted otherwise. The fetal parameters including body weight, crown-to-rump length and tail length as well as the birth outcomes including birth weight, body length and tail length were statistically calculated based on data of individual fetus. Statistical tests were performed using unpaired *t*-test using GraphPad Prism (version 5; GraphPad Software, La Jolla, CA, USA). The significance level was set at $p < 0.05$.

3. Results

3.1. Maternal exposure to CAP induces FGR in mice

To determine the impact of maternal exposure to ambient $PM_{2.5}$ on fetal development, female mice were exposed to FA or CAP during pregestational and gestational stages. At GD17.5, some pregnant mice were sacrificed to examine the intrauterine growth of fetus, and some were kept for natural delivery to check the fetal growth at birth. During the whole exposure period, the average $PM_{2.5}$ concentration in ambient air was 52.47 ± 16.74 μg/m^3, and the average $PM_{2.5}$ concentrations in FA and CAP chambers were 3.81 ± 3.38 and 217.62 ± 74.78 μg/m^3, respectively (Fig. 1**b** and **c**). Considering that the exposure was performed for 8 h/day and 5 days/week, the 24-h average $PM_{2.5}$ levels for FA- and CAP-exposed mice during the experimental period were 40.89 and 91.79 μg/m^3, respectively (as calculated by $Concentration_{ambient}X16/21 + Concentration_{chamber}X5/21$). This exposure level in CAP group was markedly higher than the national ambient air quality standards of China (35 μg/m^3), but was quite common in winter for cities with heavy air pollution such as Anyang, China. Table 2 shows that the elemental concentrations of $PM_{2.5}$ in the CAP chamber were much higher than those in FA chamber. The remarkably high concentrations of Si and S are consistent with the heavy construction and subsequent heavy transportation on campus.

Our results showed that maternal exposure to CAP did not cause significant changes of body weight in dams during pregestational or pregnancy period (Supplemental Figs. 1a and 1b). In addition, pregnancy rate or pregnancy duration was not changed by CAP exposure (data not shown). However, the weight of perirenal fat was significantly increased in CAP-exposed female mice (Table 1), while no significant changes were found in other organs including heart, liver, spleen, lung, kidney, thymus, pancreas, brain, ovary, fallopian tube, subcutaneous fat and brown fat (Table 1). Compared with FA group, CAP-exposed mice had smaller fetuses at GD17.5 (Fig. 1**d**), with the fetal weight, CRL and tail length significantly reduced by 5.8%, 4.6% and 4.5%, respectively (Fig. 1**e–g**). These differences were found in both male and female fetuses (Fig. 1**e-g**). In addition, no differences were observed for the total number of alive fetus, number of male/female fetus per litter or the sex ratio between two groups (Supplemental Fig. 1c–f). Consistent with the results at GD17.5, significant decreases in body weight, body length and tail length were also found at birth in offspring of dams exposed to CAP (for both male and female neonatal mice as demonstrated in Fig. 1**h–j**). Moreover, maternal exposure to CAP caused no change in the litter size, sex ratio or number of dead/alive male/female neonatal mice per litter (Supplemental Fig. 2a–f). Together, these results indicated that maternal exposure to CAP restricted fetal growth and induced LBW in mice, and there was no sex difference in this phenotype.

3.2. Maternal exposure to CAP disrupts placental development

Normal placental development is essential for fetal growth, and placental dysfunction has been associated with FGR. As such, we investigated the effect of maternal CAP exposure on the placental development. Our previous studies have indicated that male offspring is more prone to have developmental re-programming by maternal $PM_{2.5}$ exposure. Thus to avoid the potential influence of gender, male placentas were assessed in this study. As shown in Fig. 2**a–e**, the size of placentas from CAP-exposed dams were significantly reduced, with the minimum diameter decreased by 5.69% ($p < 0.01$), maximum diameter by 6.03% ($p < 0.01$) and surface area, an indicator of maternal-fetal nutrient transportation, by 11.34% ($p < 0.01$). H&E staining results showed no change in the cross sectional area of placentas between FA and CAP groups (Fig. 2**f–g**). However, the percentage of junctional zone was significantly downregulated in CAP-exposed mice (Fig. 2**i**).

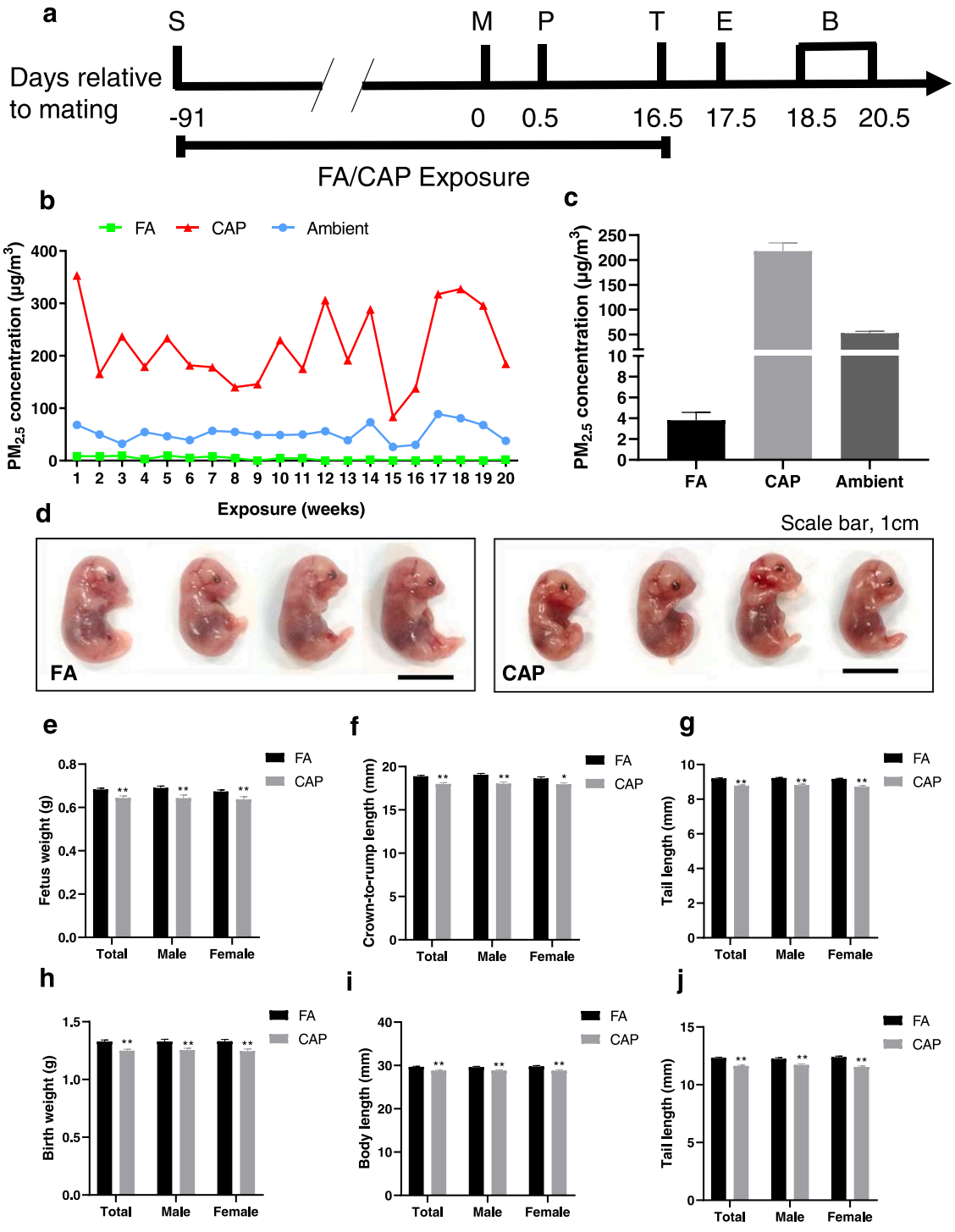

Fig. 1. Maternal exposure to CAP induces FGR in mice. a, Exposure scheme: S, start of exposure; M, mating; P, presence of sperm plug; T, termination of exposure; E, euthanization of pregnant mice; B, birth of litter. **b–c**, The $PM_{2.5}$ samples in ambient, FA and CAP chambers were collected weekly using Teflon filters and the $PM_{2.5}$ concentrations were determined by the weight differences of filters before and after exposure. **d,** Representative pictures of fetus from FA/CAP-exposed mice at GD17.5. **e–g**, Body weight (**e**), crown-to-rump length (**f**) and tail length (**g**) of fetus at GD17.5. $n = 51–65$/group. **h–j**, Body weight (**h**), body length (**i**) and tail length (**j**) of fetus at birth. $n = 69–72$/group. $^{*}p < 0.05$, $^{**}p < 0.01$ *versus* FA, unpaired *t*-test.

3.3. *Maternal exposure to CAP alters trophoblast differentiation*

Defects in development of the placenta may be caused by altered differentiation of the trophoblast lineage. To fully investigate this possibility, qPCR was performed to assess the expressions of marker genes in different lineages of trophoblast (**Summarized in** Supplemental Fig. 3). The trophectoderm gives rise to the trophoblast lineages in the placenta, and there is no difference on the expressions of Eomes and Cdx2 (Fig. 3**a** and **b**), two representative markers of the trophectoderm (Russ et al., 2000; Strumpf et al., 2005). In the meantime, the expression levels of Esx1, Gcm1, Muc1, and Syna are all significantly increased in CAP group (Fig. 3**c–f**), and all these genes are thought to be primarily or exclusively expressed in the labyrinthine/syncytiotrophoblast (SynT) (Li and Behringer, 1998; Simmons, Natale, et al., 2008; Shyu et al., 2008).

Table 1
Organ weights of pregnant mice on GD17.5.

Organs (g)	FA	CAP	*P* value
Heart	0.112 ± 0.012	0.112 ± 0.016	0.987
Liver	1.539 ± 0.176	1.467 ± 0.208	0.437
Spleen	0.081 ± 0.010	0.097 ± 0.023	0.067
Lung(left part)	0.036 ± 0.011	0.037 ± 0.002	0.824
Kidney	0.254 ± 0.027	0.265 ± 0.019	0.375
Adrenal glands	0.007 ± 0.001	0.006 ± 0.002	0.087
Skeletal muscle	0.122 ± 0.011	0.114 ± 0.012	0.155
Thymus	0.017 ± 0.003	0.017 ± 0.003	0.612
Pancreas	0.125 ± 0.015	0.131 ± 0.029	0.593
Brain	0.391 ± 0.016	0.387 ± 0.018	0.637
Ovary	0.012 ± 0.002	0.011 ± 0.003	0.560
Uterus	8.789 ± 1.67	7.535 ± 1.699	0.151
Fallopian tube	0.006 ± 0.001	0.006 ± 0.002	0.477
Parametrial fat	0.15 ± 0.038	0.19 ± 0.07	0.150
Subcutaneous fat	0.179 ± 0.05	0.193 ± 0.045	0.542
Perirenal fat	0.033 ± 0.008	0.045 ± 0.015	0.037*
Brown fat	0.042 ± 0.008	0.047 ± 0.006	0.228

$n = 10$ for FA group, $n = 8$ for CAP group.
* $p < 0.05$ *versus* FA.

Table 2
$PM_{2.5}$ samples in FA and CAP samples were collected weekly, and the elemental composition was determined by X-ray fluorescence analysis (XRF).

	FA (μg/m^3)	CAP (μg/m^3)
Na	*ND*	6.06 ± 7.33
K	0.97 ± 0.33	18.75 ± 11.62
Mg	*ND*	*ND*
Ca	*ND*	6.29 ± 4.90
Ba	*ND*	*ND*
Cd	*ND*	*ND*
Sn	0.76 ± 0.28	2.01 ± 0.30
Ti	*ND*	0.47 ± 0.00
V	*ND*	*ND*
Cr	*ND*	*ND*
Mn	*ND*	1.61 ± 0.38
Fe	*ND*	15.07 ± 2.25
Co	*ND*	*ND*
Ni	*ND*	12.94 ± 6.81
Cu	*ND*	3.86 ± 2.76
Zn	0.23 ± 0.02	8.13 ± 4.68
As	*ND*	*ND*
Se	*ND*	*ND*
Pb	*ND*	1.18 ± 0.02
Al	*ND*	2.06 ± 1.44
S	3.69 ± 0.79	90.6 ± 47.66
Sc	*ND*	*ND*
P	*ND*	0.42 ± 0.58
Si	1.51 ± 0.12	12.30 ± 2.83

ND: non-detectable.

As for the junctional zone-associated lineages (Henke et al., 2013), expression of Tpbpb was significantly reduced while that of Tpbpa was not changed (Fig. 3**g–h**). Prl3a1 and Psg17 are exclusively or predominantly expressed in the spongiotrophoblast (SpT) (Simmons, Rawn, et al., 2008; McLellan et al., 2005), while Pcdh12 is predominantly expressed in glycogen trophoblast cells (GCs) (Zheng-Fischhofer et al., 2007). Fig. 3**i–k** demonstrated that CAP exposure markedly down-regulated the expressions of Prl3a1 and Psg17, but had no effect on the expression of Pcdh12.

Furthermore, we analyzed the trophoblast giant cells (TGCs) in placenta. Expression of the bHLH transcription factor Hand1, which is essential for regulating TGCs differentiation and expressed in almost all the trophoblast giant cells (TGCs) lineages (Riley et al., 1998; Scott et al., 2000), was significantly decreased in CAP-exposed mice (Fig. 3**l**). Expression levels of Pl1 and Pl2, which are mainly expressed in parietal TGCs (P-TGCs) (Simmons et al., 2007), were both significantly decreased by CAP exposure (Fig. 3**m–n**). In addition, the expression level of Plf, which is expressed in spiral artery associated TGCs (SpA-TGCs) (Hu and Cross, 2011), was also remarkedly reduced (Fig. 3**o**). However, no difference in the expression of Ctsq (Outhwaite et al., 2015), which is expressed only in maternal sinusoidal TGCs (S-TGCs) (Fig. 3**p**), was observed between these two experimental groups.

3.4. Maternal exposure to CAP impairs spiral artery remodeling

Abnormal differentiation of trophoblast cells can influence spiral artery remodeling, which is often linked to FGR. Therefore, we further examined whether $PM_{2.5}$ exposure is associated with deficient vascular remodeling. H&E staining result revealed that CAP exposure significantly decreased the luminal area and perimeter of spiral arteries in placenta (Fig. 4**a–c**). While the ratio of total vessel area to luminal area, an indicator of spiral artery thickness, was remarkedly increased in placenta of CAP-exposed mice compared to that in FA group (Fig. 4**d**). The staining images for α-SMA confirmed that more smooth muscle cells remained in the artery wall of spiral artery in CAP-exposed mice (Fig. 4**e**). The quantitative analysis also showed that there are significantly higher proportion of α-SMA positive cells in spiral artery in CAP group compared to that in FA group (Fig. 4**f**), suggesting an insufficient remodeling of spiral artery in CAP-exposed mice.

3.5. Maternal exposure to CAP changes the levels of the placental angiogenic and angiostatic factors

Given that the formation and development of placental vascular system requires balance between angiogenic and angiostatic factors, we evaluated their expressions in the placenta at gene and protein levels after FA/CAP exposure. Compared to the FA group, CAP-exposed mice showed a significant decrease in the gene and protein expressions of VEGFA and PLGF in placenta (Fig. 5**a, b, d** and **e**), both of which are crucial angiogenic factors (Bhattacharjee et al., 2021). In addition, CAP exposure significantly increased the protein level of Flt1 (Fig. 5**f**), which is an inhibitor of vascular endothelial growth factor–mediated angiogenesis (Khankin et al., 2012). Furthermore, the gene expression of vascular endothelial growth factor receptor 2 (Flk1), which is another important VEGF receptor (Shibuya, 2013), was also significantly increased in CAP-exposed mice (Fig. 5**c**). Together, these results showed that maternal exposure to CAP disrupted the balance of placental angiogenic and angiostatic factors.

3.6. CAP exposure induces pulmonary, placental and systemic inflammation

The inflammation levels in lung, placenta and circulation were further assessed. Consistent with results from previous studies, CAP exposure induced significant inflammation in lung, the primary target organ of inhaled particulate matters, as demonstrated by increased levels of pro-inflammatory cytokines including TNFα, IL-6 and IFNγ in lung tissues (Fig. 6**a**). Time course studies have shown the precedence of pulmonary inflammation over extra-pulmonary inflammation, suggesting that $PM_{2.5}$-induced extra pulmonary inflammation such as systemic and adipose inflammation may be consequent to pulmonary inflammation. In the present study, we also found that compared with the FA group, CAP-exposed mice had significantly higher levels of systemic inflammation (increased concentrations of TNFα and MCP1 as shown in Fig. 6**b**) and placental inflammation (upregulated concentrations of inflammatory cytokines IL-6, IFNγ and IL12 (p70) as well as anti-inflammatory cytokine IL-10 as demonstrated in Fig. 6**c**). Our results suggested that inflammation may play a critical role in the development of CAP exposure-induced placental dysfunction.

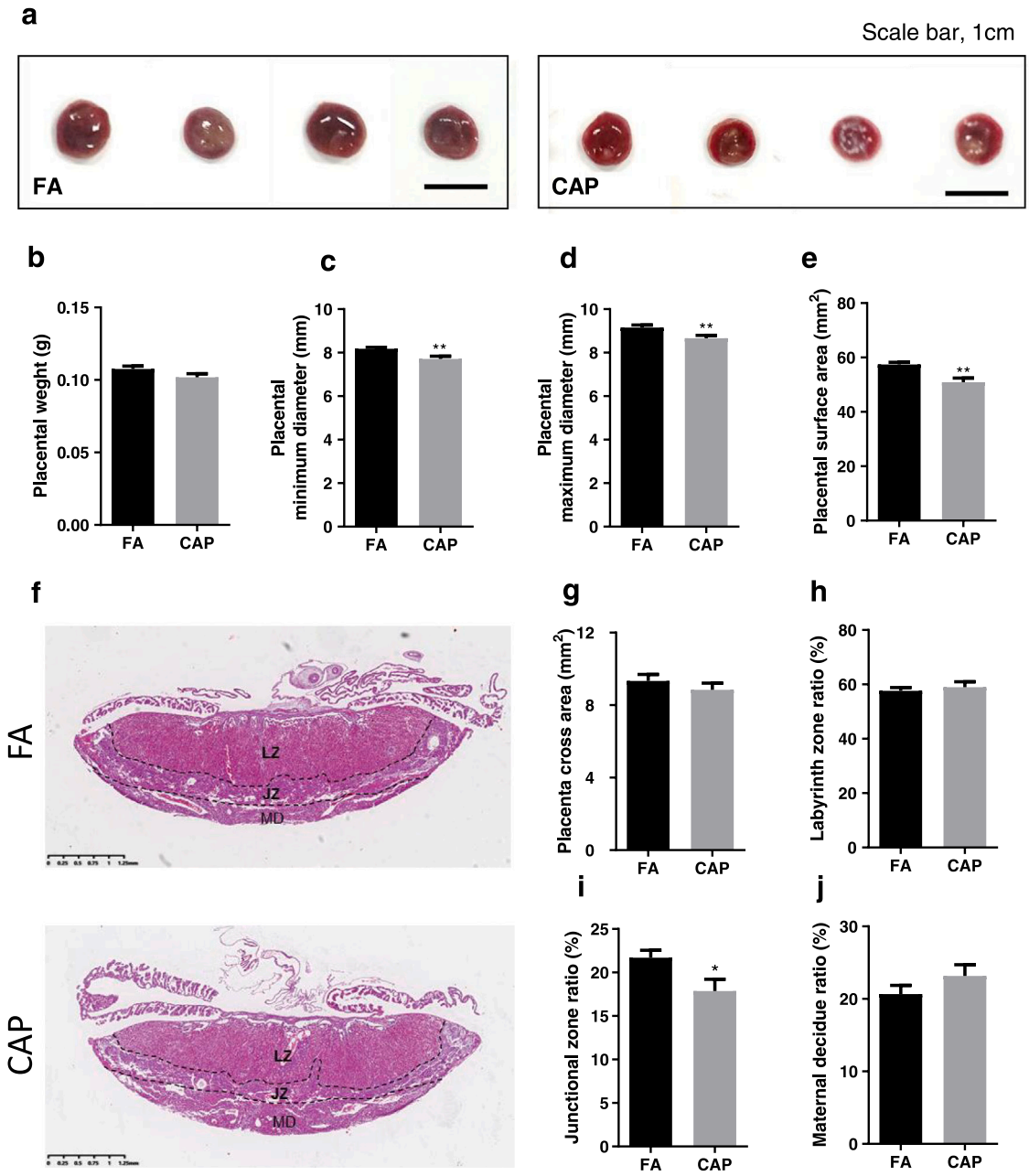

Fig. 2. Maternal exposure to CAP disrupts placental development. a, Representative images of placentas at GD17.5. **b**, Placental weight. **c–e**, minimum diameter (**c**), maximum diameter (**d**) and surface area (**e**) of placentas. $n = 28–32$/group. **f,** Representative images of H&E stained placentas. The layers of the placental architecture are labeled: labyrinth zone (LZ), junctional zone (JZ) and maternal decidual zone (DZ). **g–j,** the cross section (**g**), percentage of LZ, JZ and DZ areas in placenta. $n = 18–19$/group. $^{*}p < 0.05$, $^{**}p < 0.01$ *versus* FA, unpaired *t*-test.

4. Discussions

An increasing number of studies have suggested that maternal exposure to ambient $PM_{2.5}$ may restrict fetal growth, leading to LBW and other adverse birth outcomes (Janssen et al., 2017; Liu et al., 2007). In this study, we evaluated the effects of pregestational and gestational exposure to CAP on fetal development in utero and at birth, and investigated the placental and maternal factors which possibly participate in $PM_{2.5}$ exposure-induced fetal growth restriction. The main findings include that maternal exposure to CAP: 1) results in FGR, affects placental development and reduces the size of junctional layer; 2) inhibits the invasive TGCs differentiation, disturbs spiral artery remodeling and the angiogenic-angiostatic balance; 3) induces pulmonary, placental and systemic inflammation. These findings suggest that maternal inflammation and abnormal placental development are likely to be involved in the $PM_{2.5}$ exposure-induced FGR.

In the present study, we found that maternal exposure to $PM_{2.5}$ during pregestational and gestational stages results in LBW, and these results are in accordance with the previous studies of our research group (Chen et al., 2017; Xu et al., 2019). In addition, the body weight, body length, and tail length of fetus at GD17.5 were significantly decreased, suggesting that maternal exposure to CAP leads to FGR (Fig. 1). Further analysis demonstrated that the placental development is disturbed by CAP exposure, as manifested by significantly decreased placental size including minimum and maximum diameters and surface area (Fig. 2). Despite of a slight decrease in placental weight by CAP exposure, these results are consistent with the previous study (Soto et al., 2017). It is worth noting that CAP exposure lowered the placental surface area by

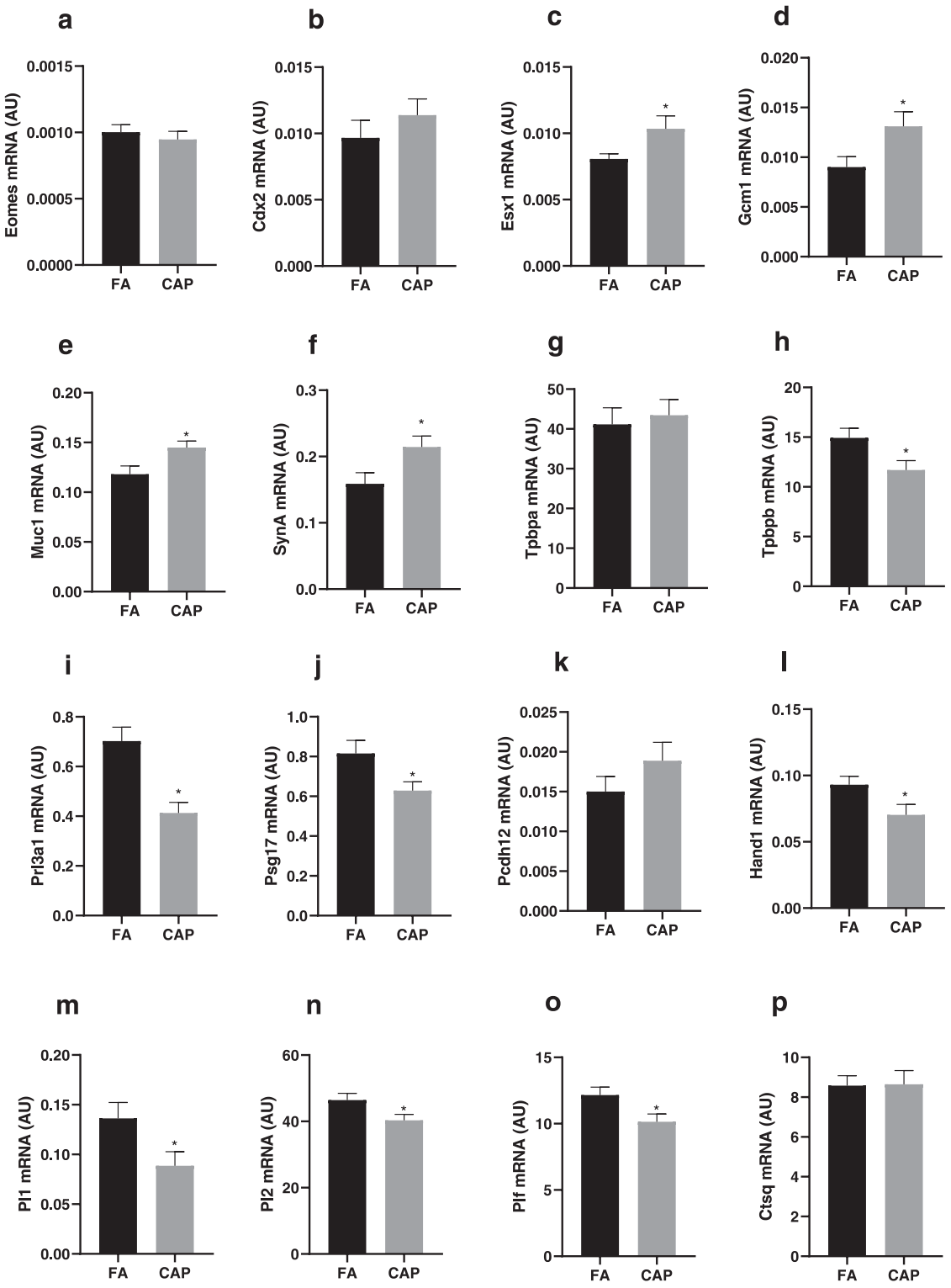

Fig. 3. Maternal exposure to CAP alters trophoblast differentiation. a–p, The mRNA expressions of Eomes (**a**), Cdx2 (**b**), Esx1 (**c**), Gcm1 (**d**), Muc1 (**e**), SynA (**f**), Tpbpa (**g**), Tpbpb (**h**), Prl3a1 (**i**), Psg17 (**j**), Pcdh12 (**k**), Hand1 (**l**), Pl1 (**m**), Pl2 (**n**), Plf (**o**) and Ctsq (**p**) of placentas were quantified by real time RT-PCR. $n = 10–13$/group, $^{*}p < 0.05$, $^{**}p < 0.01$ *versus* FA, unpaired *t*-test.

about 12%, which may have a direct or indirect effect on the capacity of the placental nutrient transportation (Fowden et al., 2006; Liu et al., 2021). The pathological histology analysis result showed that CAP exposure significantly decreases the size of junctional zone in placenta (Fig. 2). Many mouse models with a reduced thickness of the junctional layer exhibit an FGR phenotype in offspring (Saffer et al., 2013). For example, a research indicated that gestational treatment with nano-silica particles could induce FGR along with a significant decrease of placental junctional zone in mice (Levine et al., 2004). The junctional zone is composed mainly of SpT, GCs and a discontinuous layer of P-TGCs with large polyploid nuclei (Sarkar et al., 2014). qPCR analysis further demonstrated that the expression levels of SpT and P-TGC

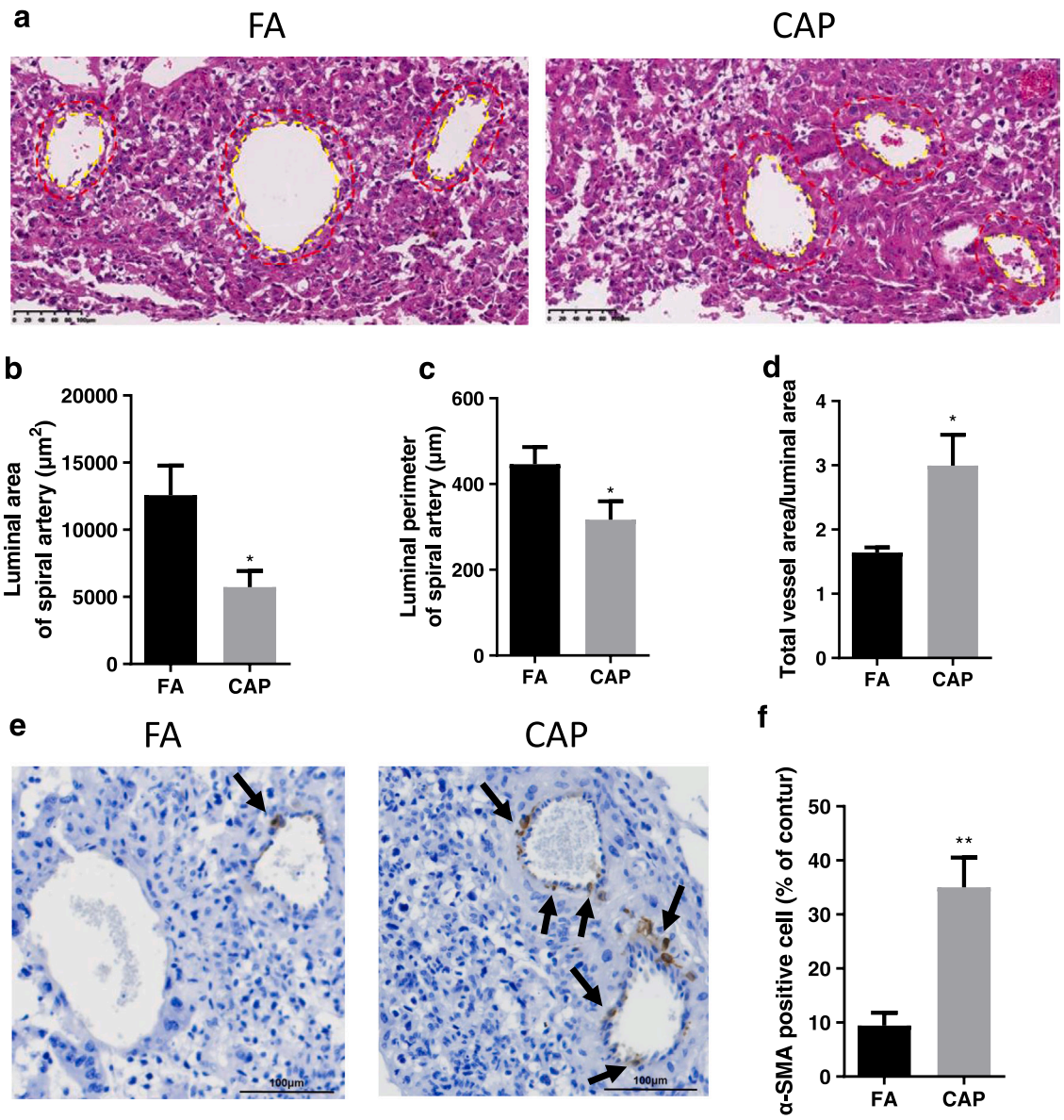

Fig. 4. Maternal exposure to CAP impairs spiral artery remodeling. a, Representative H&E images of the spiral arteries in the decidual zone in placentas from FA/CAP group, red dashed line: total vessel area, yellow dashed line: lumen area. **b–d**, Quantification of luminal areas (**b**), luminal perimeter (**c**) and ratio of total vessel area to luminal area (**d**) of spiral artery. **e,** Representative α-SMA staining images, the VSMCs around the spiral artery are labeled, black arrowhead: positive staining cells. **f**, Quantification of α-SMA-positive cells around the spiral artery. $n = 18$–19/group, $^{*}p < 0.05$, $^{**}p < 0.01$ *versus* FA, unpaired *t*-test.

markers are both significantly decreased in placenta from CAP-exposed mice (Fig. 3), suggesting that the reduced junctional zone may result from the reduced number of SpT and P-TGC. Therefore, these results indicated that maternal exposure to $PM_{2.5}$ may induce FGR by disrupting the development of placenta.

Abnormal spiral artery remodeling is considered to be an etiology and defining feature of obstetric complications such as FGR and pre-eclampsia (Vinay and Kwon, 2012; Alijotas-Reig et al., 2017; Zhao et al., 2015). In the present study, we also found that maternal CAP exposure disrupted the spiral artery remodeling, as indicated by the narrowed vascular lumen and thickened vascular wall accompanied by more residual VSMCs in artery (Fig. 4). Disturbance in this process may limit the maternal blood supply to the placenta and thereby restricting the fetal development. An increasing number of epidemiological studies have indicated a linkage between maternal exposure to $PM_{2.5}$ and pre-eclampsia (Yu et al., 2020), which is mainly caused by abnormal spiral artery remodeling. Trophoblast cells particularly TGCs are thought to be crucial in the process of spiral artery remodeling because of their invasive properties. As an important type of TGCs, SpA-TGC is generally thought to increase maternal blood flow to the implantation site by invading into the lumen of spiral arteries (Simmons et al., 2007). Researches have demonstrated that reduction of SpA-TGC is associated with defects in maternal spiral artery remodeling in the mouse placenta (Hu and Cross, 2011). In this study, we found that CAP exposure significantly decreased the expression levels of SpA-TGC markers (Fig. 3), indicating that there may be a decreased number of SpA-TGC. In addition, spiral artery remodeling requires adequate and organized interaction of angiogenic factors (such as VEGF and PLGF) and their receptors (VEGF and PLGF can act through the FLT1 and FLK1 (Gilbert et al., 2007; Levine et al., 2006)). Consistent with spiral artery remodeling result, our data showed that CAP exposure significantly decreased VEGF in placenta at both gene and protein levels, which is in agreement with previous study (Soto et al., 2017). In addition, the mRNA and protein levels of PLGF, another important angiogenic factor participating in spiral artery remodeling (Saffer et al., 2013), were also significantly decreased in placenta after CAP exposure. Meanwhile, CAP

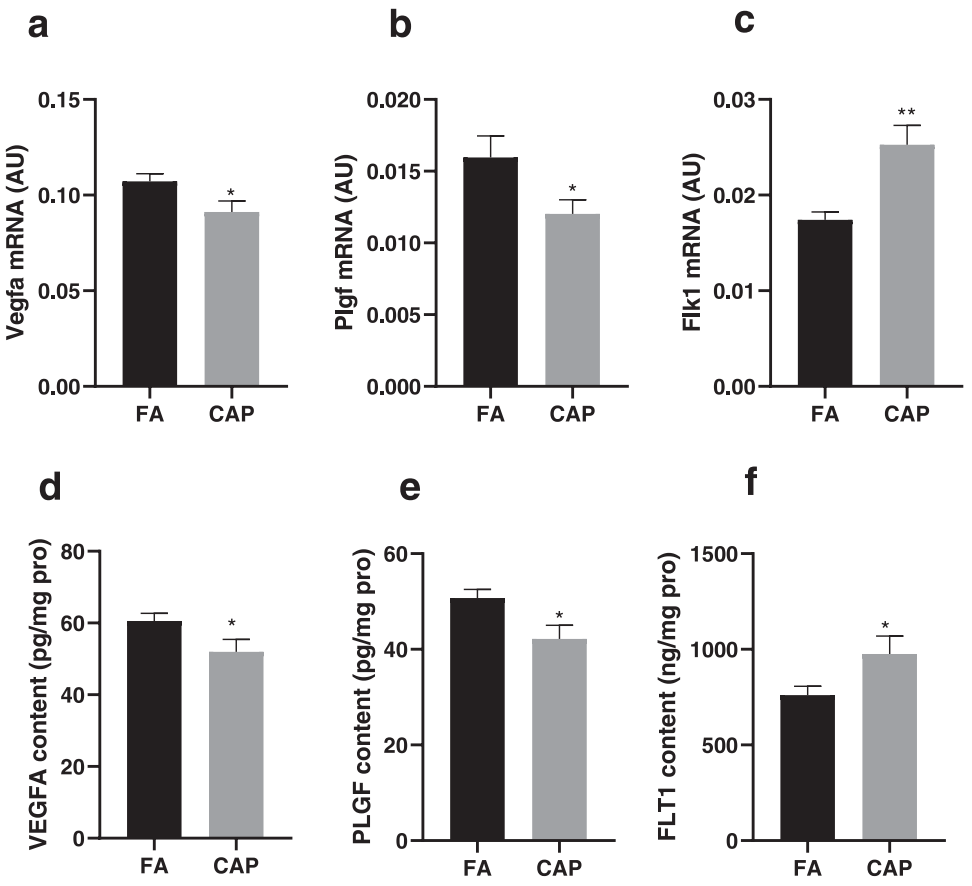

Fig. 5. Maternal exposure to CAP changes levels of the placental angiogenic and angiostatic factors. a–c, The mRNA expressions of Vegfa (**a**), Plgf (**b**) and Flk1 (**c**) in placenta. **d–f**, The protein levels of VEGFA (**d**), PLGF (**e**) and FLT1 (**f**) in placenta. $n = 10–13$/group, $^{*}p < 0.05$, $^{**}p < 0.01$ *versus* FA, unpaired *t*-test.

exposure significantly increased the expression levels of two VEGF receptors FLT1 and FLK1. Specifically, FLT1 is thought to be capable of combing with VEGF and PLGF to inhibit their biological functions and disturb the placental vascular development (Shibuya, 2013; Levine et al., 2004). Epidemiological studies have shown that the placental FLT1 level was elevated in patients with preeclampsia (Maynard et al., 2003). Toxicological studies also found that abnormal spiral artery remodeling is associated with the upregulation of FLT1 levels in animal models (Fan et al., 2014). Together with these result, our study indicated that $PM_{2.5}$ exposure induces the abnormal spiral artery remodeling *via* the disruption of placental angiogenesis.

The mechanism by which $PM_{2.5}$ exposure impairs placental development is unclear. In this study, our results demonstrated that CAP exposure significantly increased the protein levels of pro-inflammatory cytokines including IL-6, IL-12 (p70) and IFNγ in placenta, suggesting that CAP exposure induced the inflammation response in placenta. It is found that pronounced pulmonary inflammation induced by inhaled $PM_{2.5}$ lead to subsequent systemic inflammatory response, which may be the primary cause of inflammation within extra pulmonary organs. In the present study, as expected, we found that CAP exposure significantly increased the levels of several inflammatory cytokines in the lung and serum (Fig. 6). It is interesting to note that the protein level of TNFα were both dramatically increased in the lung and serum after CAP exposure. This result may indicate that $PM_{2.5}$ exposure stimulates the production of TNFα in the lung, which then further released into the bloodstream. TNFα is one of the prototype pro-inflammatory cytokine and a crucial component of inflammatory responses (Vinay and Kwon, 2012), which can cause cellular dysfunction through multiple mechanisms such as NF-κB activation (Alijotas-Reig et al., 2017; Zhao et al., 2015). During pregnancy, abnormal TNFα expression has detrimental effects on trophoblast cells and vascular development in placenta. It is found that the serum levels of TNFα in women with preeclampsia are significantly higher than those with normal pregnancies (Alijotas-Reig et al., 2017; Conrad et al., 1998; Kim et al., 2017; Cindrova-Davies et al., 2007). Further investigation indicated that administration of TNFα synthesis inhibitor could reverse LPS-induced TNFα production and fetal intra-uterine growth restriction in mice (Xu et al., 2006). In addition, *in vitro* studies have shown that TNFα increased oxidative stress and apoptosis of human primary trophoblasts through NF-κB activation (Wang et al., 2020). Thus, our findings suggest that $PM_{2.5}$ exposure induces pulmonary inflammation, which then cause systemic and placental inflammation, finally leading to placental dysfunction and FGR.

5. Conclusions

In summary, the present study demonstrated that maternal exposure to CAP induced pulmonary and extra-pulmonary inflammation, altered trophoblast lineage differentiation and disrupted the placental angiogenesis process, which then inhibited the development of junctional zone and spiral artery remodeling, leading to FGR. These data not only call special attentions to the protection of women from $PM_{2.5}$ exposure, but also give some insights into the potential molecular mechanisms of FGR and LBW caused by ambient $PM_{2.5}$.

Ethics approval and consent to participate

Not applicable.

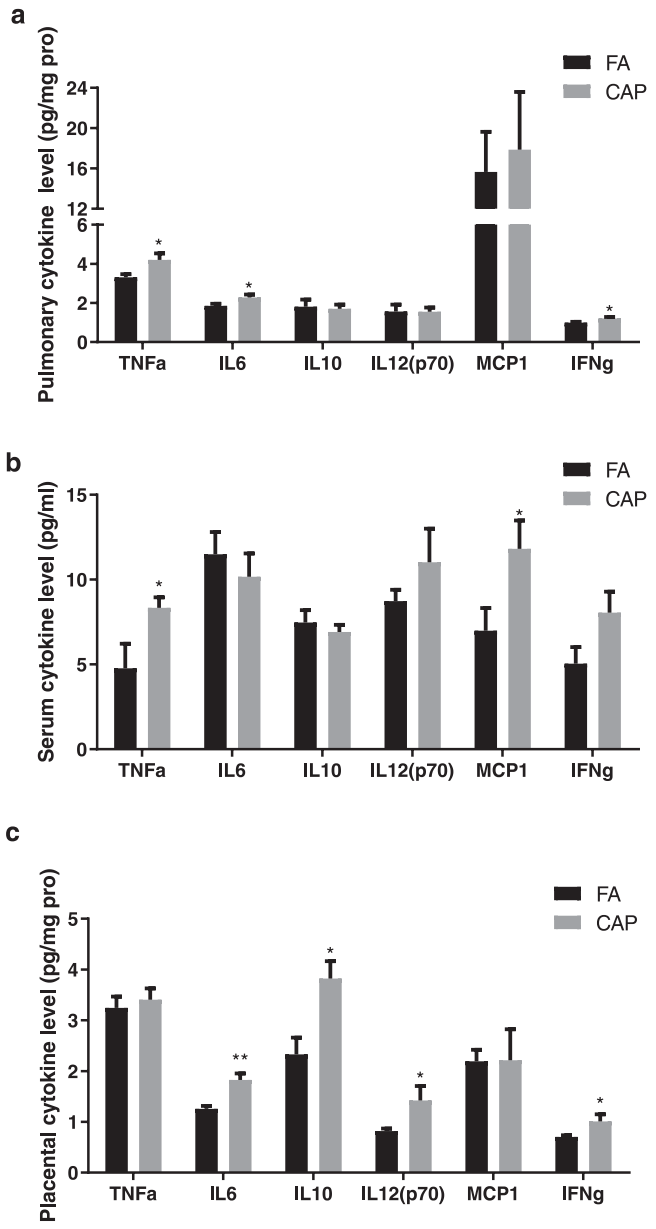

Fig. 6. CAP exposure induces pulmonary, placental and systemic inflammation. a–c, The levels of inflammatory cytokines including TNFα, IL6, IL10, IL12 (p70), MCP1 and IFNγ in lung (**a**), placenta (**b**) and circulation (**c**) of FA/CAP-exposed mice. $n = 8$–10/group, $^{*}p < 0.05$, $^{**}p < 0.01$ *versus* FA, unpaired *t*-test.

Funding

This work was supported by the National Key Research and Development Program of China (2019YFC1804503 to YX), the National Natural Science Foundation of China (Grant No. 82003414 to YX, 81873834 to XZ) and the Shanghai Municipal Science and Technology Commission (21S11901000 to WL).

CRediT authorship contribution statement

Shimin Tao: Methodology, Data curation, Formal analysis, Wring-original Draft. **Xuan Zhang:** Methodology, Formal analysis, Wring-original Draft, Funding acquisition. **Fang Tian:** Data curation, Formal analysis, Methodology. **Bin Pan:** Formal analysis, Validation. **Renzhen Peng:** Formal analysis, Validation. **Yuzhu Wang:** Methodology, Validation. **Minjie Xia:** Methodology, Validation. **Minjun Yang:** Methodology, Validation. **Jingying Hu:** Methodology, Validation. **Haidong Kan:** Conceptualization, Resources. **Yanyi Xu:** Conceptualization, Writing-Original Draft, Writing-Review & Editing, Project administration, Funding acquisition. **Weihua Li:** Conceptualization, Writing-Review & Editing, Supervision, Funding acquisition.

Declaration of Competing Interest

The authors declare the following financial interests/personal relationships which may be considered as potential competing interests: Yanyi Xu reports financial support was provided by National Key Research and Development Program of China. Yanyi Xu, Xuan Zhang reports financial support was provided by National Natural Science Foundation of China. Weihua Li reports financial support was provided by Shanghai Municipal Science and Technology Commission.

Availability of data and materials

The datasets used and/or analyzed during the present study are available from the corresponding author on reasonable request.

Acknowledgements

Not applicable.

Authors' contributions

ST, XZ, BP, RP, YW and MX acquired and analyzed the data used in the present study. ST, YX, FT, MY and JH analyzed and interpreted the present results. ST, XZ, YX and WL drafted the manuscript. HK were also major contributors in writing the manuscript. All authors read and approved the final manuscript.

Consent for publication

Not applicable.

Competing Interest

Not applicable.

Appendix A. Supporting information

Supplementary data associated with this article can be found in the online version at doi:10.1016/j.ecoenv.2022.113512.

References

Alijotas-Reig, J., Esteve-Valverde, E., Ferrer-Oliveras, R., Llurba, E., Gris, J.M., 2017. Tumor necrosis factor-alpha and pregnancy: focus on biologics. an updated and comprehensive review. Clin Rev Allergy Immunol 53 (1), 40–53. https://doi.org/10.1007/s12016-016-8596-x. ⟨https://www.ncbi.nlm.nih.gov/pubmed/28054230⟩.

Bhattacharjee, J., Mohammad, S., Goudreau, A.D., Adamo, K.B., 2021. Physical activity differentially regulates VEGF, PlGF, and their receptors in the human placenta. Physiol. Rep. 9 (2), e14710 https://doi.org/10.14814/phy2.14710. ⟨https://www.ncbi.nlm.nih.gov/pubmed/33463910⟩.

Blum, J.L., Xiong, J.Q., Hoffman, C., Zelikoff, J.T., 2012. Cadmium associated with inhaled cadmium oxide nanoparticles impacts fetal and neonatal development and growth. Toxicol. Sci. 126 (2), 478–486. https://doi.org/10.1093/toxsci/kfs008. ⟨https://www.ncbi.nlm.nih.gov/pubmed/22240978⟩.

Blum, J.L., Chen, L.C., Zelikoff, J.T., 2017. Exposure to ambient particulate matter during specific gestational periods produces adverse obstetric consequences in mice. Environ. Health Perspect. 125 (7), 077020 https://doi.org/10.1289/EHP1029. ⟨https://www.ncbi.nlm.nih.gov/pubmed/28893721⟩.

Brosens, I., Pijnenborg, R., Vercruysse, L., Romero, R., 2011. The "great obstetrical syndromes" are associated with disorders of deep placentation. Am. J. Obstet. Gynecol. 204 (3), 193–201. https://doi.org/10.1016/j.ajog.2010.08.009. ⟨https://www.ncbi.nlm.nih.gov/pubmed/21094932⟩.

Burton, G.J., Fowden, A.L., Thornburg, K.L., 2016. Placental origins of chronic disease. Physiol. Rev. 96 (4), 1509–1565. https://doi.org/10.1152/physrev.00029.2015. ⟨https://www.ncbi.nlm.nih.gov/pubmed/27604528⟩.

Chen, M., Wang, X., Hu, Z., Zhou, H., Xu, Y., Qiu, L., et al., 2017. Programming of mouse obesity by maternal exposure to concentrated ambient fine particles. Part Fibre Toxicol. 14 (1), 20. https://doi.org/10.1186/s12989-017-0201-9. ⟨https://www.ncbi.nlm.nih.gov/pubmed/28645299⟩.

Chen, R., Yin, P., Meng, X., Liu, C., Wang, L., Xu, X., et al., 2017. Fine particulate air pollution and daily mortality. A nationwide analysis in 272 Chinese cities. Am. J. Respir. Crit. Care Med. 196 (1), 73–81. https://doi.org/10.1164/rccm.201609-1862OC. ⟨https://www.ncbi.nlm.nih.gov/pubmed/28248546⟩.

Cindrova-Davies, T., Spasic-Boskovic, O., Jauniaux, E., Charnock-Jones, D.S., Burton, G. J., 2007. Nuclear factor-kappa B, p38, and stress-activated protein kinase mitogen-activated protein kinase signaling pathways regulate proinflammatory cytokines and apoptosis in human placental explants in response to oxidative stress: effects of antioxidant vitamins. Am. J. Pathol. 170 (5), 1511–1520. https://doi.org/10.2353/ajpath.2007.061035. ⟨https://www.ncbi.nlm.nih.gov/pubmed/17456758⟩.

Conrad, K.P., Miles, T.M., Benyo, D.F., 1998. Circulating levels of immunoreactive cytokines in women with preeclampsia. Am. J. Reprod. Immunol. 40 (2), 102–111. https://doi.org/10.1111/j.1600-0897.1998.tb00398.x. ⟨https://www.ncbi.nlm.nih.gov/pubmed/9764352⟩.

Familari, M., Naav, A., Erlandsson, L., de Iongh, R.U., Isaxon, C., Strandberg, B., et al., 2019. Exposure of trophoblast cells to fine particulate matter air pollution leads to growth inhibition, inflammation and ER stress. PLoS One 14 (7), e0218799. https://doi.org/10.1371/journal.pone.0218799. ⟨https://www.ncbi.nlm.nih.gov/pubmed/31318865⟩.

Fan, X., Rai, A., Kambham, N., Sung, J.F., Singh, N., Petitt, M., et al., 2014. Endometrial VEGF induces placental sFLT1 and leads to pregnancy complications. J. Clin. Invest. 124 (11), 4941–4952. https://doi.org/10.1172/JCI76864. ⟨https://www.ncbi.nlm.nih.gov/pubmed/25329693⟩.

Fowden, A.L., Ward, J.W., Wooding, F.P., Forhead, A.J., Constancia, M., 2006. Programming placental nutrient transport capacity. J. Physiol. 572 (Pt 1), 5–15. https://doi.org/10.1113/jphysiol.2005.104141. ⟨https://www.ncbi.nlm.nih.gov/pubmed/16439433⟩.

Gilbert, J.S., Babcock, S.A., Granger, J.P., 2007. Hypertension produced by reduced uterine perfusion in pregnant rats is associated with increased soluble fms-like tyrosine kinase-1 expression. Hypertension 50 (6), 1142–1147. https://doi.org/10.1161/HYPERTENSIONAHA.107.096594. ⟨https://www.ncbi.nlm.nih.gov/pubmed/17923588⟩.

Gluckman, P.D., Hanson, M.A., Cooper, C., Thornburg, K.L., 2008. Effect of in utero and early-life conditions on adult health and disease. N. Engl. J. Med. 359 (1), 61–73. https://doi.org/10.1056/NEJMra0708473. ⟨https://www.ncbi.nlm.nih.gov/pubmed/18596274⟩.

Henke, C., Ruebner, M., Faschingbauer, F., Stolt, C.C., Schaefer, N., Lang, N., et al., 2013. Regulation of murine placentogenesis by the retroviral genes Syncytin-A, Syncytin-B and Peg10. Differentiation 85 (4–5), 150–160. https://doi.org/10.1016/j.diff.2013.02.002. ⟨https://www.ncbi.nlm.nih.gov/pubmed/23807393⟩.

Hu, D., Cross, J.C., 2011. Ablation of Tpbpa-positive trophoblast precursors leads to defects in maternal spiral artery remodeling in the mouse placenta. Dev. Biol. 358 (1), 231–239. https://doi.org/10.1016/j.ydbio.2011.07.036. ⟨https://www.ncbi.nlm.nih.gov/pubmed/21839735⟩.

Janssen, B.G., Saenen, N.D., Roels, H.A., Madhloum, N., Gyselaers, W., Lefebvre, W., et al., 2017. Fetal thyroid function, birth weight, and in utero exposure to fine particle air pollution: a birth cohort study. Environ. Health Perspect. 125 (4), 699–705. https://doi.org/10.1289/EHP508. ⟨https://www.ncbi.nlm.nih.gov/pubmed/27623605⟩.

Khankin, E.V., Mandala, M., Colton, I., Karumanchi, S.A., Osol, G., 2012. Hemodynamic, vascular, and reproductive impact of FMS-like tyrosine kinase 1 (FLT1) blockade on the uteroplacental circulation during normal mouse pregnancy. Biol. Reprod. 86 (2), 57. https://doi.org/10.1095/biolreprod.111.095380. ⟨https://www.ncbi.nlm.nih.gov/pubmed/22075472⟩.

Kim, J., Lee, K.S., Kim, J.H., Lee, D.K., Park, M., Choi, S., et al., 2017. Aspirin prevents TNF-alpha-induced endothelial cell dysfunction by regulating the NF-kappaB-dependent miR-155/eNOS pathway: role of a miR-155/eNOS axis in preeclampsia. Free Radic. Biol. Med. 104, 185–198. https://doi.org/10.1016/j.freeradbiomed.2017.01.010. ⟨https://www.ncbi.nlm.nih.gov/pubmed/28087411⟩.

Levine, R.J., Maynard, S.E., Qian, C., Lim, K.H., England, L.J., Yu, K.F., et al., 2004. Circulating angiogenic factors and the risk of preeclampsia. N. Engl. J. Med. 350 (7), 672–683. https://doi.org/10.1056/NEJMoa031884. ⟨https://www.ncbi.nlm.nih.gov/pubmed/14764923⟩.

Levine, R.J., Lam, C., Qian, C., Yu, K.F., Maynard, S.E., Sachs, B.P., 2006. Soluble endoglin and other circulating antiangiogenic factors in preeclampsia. N. Engl. J. Med. 355 (10), 992–1005. https://doi.org/10.1056/NEJMoa055352. ⟨https://www.ncbi.nlm.nih.gov/pubmed/16957146⟩.

Li, Y., Behringer, R.R., 1998. Esx1 is an X-chromosome-imprinted regulator of placental development and fetal growth. Nat. Genet. 20 (3), 309–311. https://doi.org/10.1038/3129. ⟨https://www.ncbi.nlm.nih.gov/pubmed/9806555⟩.

Liu, H.J., Liu, P.C., Hua, J., Zhao, Y., Cao, J., 2021. Placental weight and size in relation to fetal growth restriction: a case-control study. J. Matern. Fetal Neonatal. Med. 34 (9), 1356–1360. https://doi.org/10.1080/14767058.2019.1636371. ⟨https://www.ncbi.nlm.nih.gov/pubmed/31234675⟩.

Liu, S., Krewski, D., Shi, Y., Chen, Y., Burnett, R.T., 2007. Association between maternal exposure to ambient air pollutants during pregnancy and fetal growth restriction. J. Expo. Sci. Environ. Epidemiol. 17 (5), 426–432. https://doi.org/10.1038/sj.jes.7500503. ⟨https://www.ncbi.nlm.nih.gov/pubmed/16736056⟩.

Maynard, S.E., Min, J.Y., Merchan, J., Lim, K.H., Li, J., Mondal, S., et al., 2003. Excess placental soluble fms-like tyrosine kinase 1 (sFlt1) may contribute to endothelial dysfunction, hypertension, and proteinuria in preeclampsia. J. Clin. Invest. 111 (5), 649–658. https://doi.org/10.1172/JCI17189. ⟨https://www.ncbi.nlm.nih.gov/pubmed/12618519⟩.

McLellan, A.S., Fischer, B., Dveksler, G., Hori, T., Wynne, F., Ball, M., 2005. Structure and evolution of the mouse pregnancy-specific glycoprotein (Psg) gene locus. BMC Genom. 6, 4. https://doi.org/10.1186/1471-2164-6-4. ⟨https://www.ncbi.nlm.nih.gov/pubmed/15647114⟩.

Muller, J.E., Meyer, N., Santamaria, C.G., Schumacher, A., Luque, E.H., Zenclussen, M.L., et al., 2018. Bisphenol A exposure during early pregnancy impairs uterine spiral artery remodeling and provokes intrauterine growth restriction in mice. Sci. Rep. 8 (1), 9196. https://doi.org/10.1038/s41598-018-27575-y. ⟨https://www.ncbi.nlm.nih.gov/pubmed/29907759⟩.

Murray, C.J.L., Aravkin, A.Y., Zheng, P., Abbafati, C., Abbas, K.M., Abbasi-Kangevari, M., et al., 2020M. Global burden of 87 risk factors in 204 countries and territories, 1990–2019: a systematic analysis for the Global Burden of Disease Study 2019. Lancet 396 (10258), 1223–1249. https://doi.org/10.1016/s0140-6736(20)30752–2.

Naav, A., Erlandsson, L., Isaxon, C., Asander Frostner, E., Ehinger, J., Sporre, M.K., et al., 2020. Urban PM2.5 induces cellular toxicity, hormone dysregulation, oxidative damage, inflammation, and mitochondrial interference in the HRT8 trophoblast cell line. Front. Endocrinol. 11 (75) https://doi.org/10.3389/fendo.2020.00075. ⟨https://www.ncbi.nlm.nih.gov/pubmed/32226408⟩.

Nel, A., 2005. Atmosphere. Air pollution-related illness: effects of particles. Science 308 (5723), 804–806. https://doi.org/10.1126/science.1108752, 804-0. ⟨https://www.ncbi.nlm.nih.gov/pubmed/15879201⟩.

Outhwaite, J.E., McGuire, V., Simmons, D.G., 2015. Genetic ablation of placental sinusoidal trophoblast giant cells causes fetal growth restriction and embryonic lethality. Placenta 36 (8), 951–955. https://doi.org/10.1016/j.placenta.2015.05.013. ⟨https://www.ncbi.nlm.nih.gov/pubmed/26091829⟩.

Przybyl, L., Haase, N., Golic, M., Rugor, J., Solano, M.E., Arck, P.C., 2016. CD74-downregulation of placental macrophage-trophoblastic interactions in preeclampsia. Circ. Res. 119 (1), 55–68. https://doi.org/10.1161/CIRCRESAHA.116.308304. ⟨https://www.ncbi.nlm.nih.gov/pubmed/27199465⟩.

Riley, P., Anson-Cartwright, L., Cross, J.C., 1998. The Hand1 bHLH transcription factor is essential for placentation and cardiac morphogenesis. Nat. Genet. 18 (3), 271–275. https://doi.org/10.1038/ng0398-271. ⟨https://www.ncbi.nlm.nih.gov/pubmed/9500551⟩.

Russ, A.P., Wattler, S., Colledge, W.H., Aparicio, S.A., Carlton, M.B., Pearce, J.J., 2000. Eomesodermin is required for mouse trophoblast development and mesoderm formation. Nature 404 (6773), 95–99. https://doi.org/10.1038/35003601. ⟨https://www.ncbi.nlm.nih.gov/pubmed/10716450⟩.

Saffer, C., Olson, G., Boggess, K.A., Beyerlein, R., Eubank, C., Sibai, B.M., et al., 2013. Determination of placental growth factor (PlGF) levels in healthy pregnant women without signs or symptoms of preeclampsia. Pregnancy Hypertens. 3 (2), 124–132. https://doi.org/10.1016/j.preghy.2013.01.004. ⟨https://www.ncbi.nlm.nih.gov/pubmed/26105949⟩.

Sarkar, A.A., Nuwayhid, S.J., Maynard, T., Ghandchi, F., Hill, J.T., Lamantia, A.S., et al., 2014. Hectd1 is required for development of the junctional zone of the placenta. Dev. Biol. 392 (2), 368–380. https://doi.org/10.1016/j.ydbio.2014.05.007. ⟨https://www.ncbi.nlm.nih.gov/pubmed/24855001⟩.

Scott, I.C., Anson-Cartwright, L., Riley, P., Reda, D., Cross, J.C., 2000. The HAND1 basic helix-loop-helix transcription factor regulates trophoblast differentiation via multiple mechanisms. Mol. Cell. Biol. 20 (2), 530–541. https://doi.org/10.1128/MCB.20.2.530-541.2000. ⟨https://www.ncbi.nlm.nih.gov/pubmed/10611232⟩.

Shaddick, G., Thomas, M.L., Mudu, P., Ruggeri, G., Gumy, S., 2020. Half the world's population are exposed to increasing air pollution. Npj Clim. Atmos. Sci. 3, 1. https://doi.org/10.1038/s41612-020-0124-2 (doi:ARTN23. ://WOS:000540768100001).

Sharma, D., Farahbakhsh, N., Shastri, S., Sharma, P., 2016. Intrauterine growth restriction – Part 2. J. Matern. Fetal Neonatal. Med. 29 (24), 4037–4048. https://doi.org/10.3109/14767058.2016.1154525. ⟨https://www.ncbi.nlm.nih.gov/pubmed/26979578⟩.

Sharma, D., Shastri, S., Sharma, P., 2016. Intrauterine growth restriction: antenatal and postnatal aspects. Clin. Med. Insights Pediatr. 10, 67–83. https://doi.org/10.4137/CMPed.S40070. ⟨https://www.ncbi.nlm.nih.gov/pubmed/27441006⟩.

Shibuya, M., 2013. Vascular endothelial growth factor and its receptor system: physiological functions in angiogenesis and pathological roles in various diseases. J. Biochem. 153 (1), 13–19. https://doi.org/10.1093/jb/mvs136. ⟨https://www.ncbi.nlm.nih.gov/pubmed/23172303⟩.

Shyu, M.K., Lin, M.C., Liu, C.H., Fu, Y.R., Shih, J.C., Lee, C.N., 2008. MUC1 expression is increased during human placental development and suppresses trophoblast-like cell invasion in vitro. Biol. Reprod. 79 (2), 233–239. https://doi.org/10.1095/biolreprod.108.067629. ⟨https://www.ncbi.nlm.nih.gov/pubmed/18417712⟩.

Simmons, D.G., Fortier, A.L., Cross, J.C., 2007. Diverse subtypes and developmental origins of trophoblast giant cells in the mouse placenta. Dev. Biol. 304 (2), 567–578. https://doi.org/10.1016/j.ydbio.2007.01.009. ⟨https://www.ncbi.nlm.nih.gov/pubmed/17289015⟩.

Simmons, D.G., Natale, D.R., Begay, V., Hughes, M., Leutz, A., Cross, J.C., 2008. Early patterning of the chorion leads to the trilaminar trophoblast cell structure in the placental labyrinth. Development 135 (12), 2083–2091. https://doi.org/10.1242/dev.020099. ⟨https://www.ncbi.nlm.nih.gov/pubmed/18448564⟩.

Simmons, D.G., Rawn, S., Davies, A., Hughes, M., Cross, J.C., 2008. Spatial and temporal expression of the 23 murine prolactin/placental lactogen-related genes is not associated with their position in the locus. BMC Genom. 9, 352. https://doi.org/10.1186/1471-2164-9-352. ⟨https://www.ncbi.nlm.nih.gov/pubmed/18662396⟩.

Soto, S.F., Melo, J.O., Marchesi, G.D., Lopes, K.L., Veras, M.M., Oliveira, I.B., 2017. Exposure to fine particulate matter in the air alters placental structure and the renin-angiotensin system. PLoS One 12 (8), e0183314. https://doi.org/10.1371/journal.pone.0183314. ⟨https://www.ncbi.nlm.nih.gov/pubmed/28820906⟩.

Strumpf, D., Mao, C.A., Yamanaka, Y., Ralston, A., Chawengsaksophak, K., Beck, F., 2005. Cdx2 is required for correct cell fate specification and differentiation of trophectoderm in the mouse blastocyst. Development 132 (9), 2093–2102. https://doi.org/10.1242/dev.01801. ⟨https://www.ncbi.nlm.nih.gov/pubmed/15788452⟩.

Tewari, N., Kalkunte, S., Murray, D.W., Sharma, S., 2009. The water channel aquaporin 1 is a novel molecular target of polychlorinated biphenyls for in utero anomalies. J. Biol. Chem. 284 (22), 15224–15232. https://doi.org/10.1074/jbc.M808892200. ⟨https://www.ncbi.nlm.nih.gov/pubmed/19332547⟩.

Veras, M.M., Damaceno-Rodrigues, N.R., Caldini, E.G., Maciel Ribeiro, A.A., Mayhew, T. M., Saldiva, P.H., et al., 2008. Particulate urban air pollution affects the functional morphology of mouse placenta. Biol. Reprod. 79 (3), 578–584. https://doi.org/10.1095/biolreprod.108.069591. ⟨https://www.ncbi.nlm.nih.gov/pubmed/18509159⟩.

Vinay, D.S., Kwon, B.S., 2012. Targeting TNF superfamily members for therapeutic intervention in rheumatoid arthritis. Cytokine 57 (3), 305–312. https://doi.org/10.1016/j.cyto.2011.12.005. ⟨https://www.ncbi.nlm.nih.gov/pubmed/22209079⟩.

Wang, Z., Zibrila, A.I., Liu, S., Zhao, G., Li, Y., Xu, J., et al., 2020. Acetylcholine ameliorated TNF-alpha-induced primary trophoblast malfunction via muscarinic receptorsdagger. Biol. Reprod. 103 (6), 1238–1248. https://doi.org/10.1093/biolre/ioaa158. ⟨https://www.ncbi.nlm.nih.gov/pubmed/32902620⟩.

Xu, D.X., Chen, Y.H., Wang, H., Zhao, L., Wang, J.P., Wei, W., 2006. Tumor necrosis factor alpha partially contributes to lipopolysaccharide-induced intra-uterine fetal growth restriction and skeletal development retardation in mice. Toxicol. Lett. 163 (1), 20–29. https://doi.org/10.1016/j.toxlet.2005.09.009. ⟨https://www.ncbi.nlm.nih.gov/pubmed/16263228⟩.

Xu, Y., Wang, W., Chen, M., Zhou, J., Huang, X., Tao, S., 2019. Developmental programming of obesity by maternal exposure to concentrated ambient PM2.5 is maternally transmitted into the third generation in a mouse model. Part Fibre Toxicol. 16 (1), 27. https://doi.org/10.1186/s12989-019-0312-6. ⟨https://www.ncbi.nlm.nih.gov/pubmed/31266526⟩.

Ying, Z., Xu, X., Bai, Y., Zhong, J., Chen, M., Liang, Y., 2014. Long-term exposure to concentrated ambient PM2.5 increases mouse blood pressure through abnormal activation of the sympathetic nervous system: a role for hypothalamic inflammation. Environ. Health Perspect. 122 (1), 79–86. https://doi.org/10.1289/ehp.1307151. ⟨https://www.ncbi.nlm.nih.gov/pubmed/24240275⟩.

Yu, H., Yin, Y., Zhang, J., Zhou, R., 2020. The impact of particulate matter 2.5 on the risk of preeclampsia: an updated systematic review and meta-analysis. Environ. Sci. Pollut. Res. Int. 27 (30), 37527–37539. https://doi.org/10.1007/s11356-020-10112-8. ⟨https://www.ncbi.nlm.nih.gov/pubmed/32740838⟩.

Yue, H., Ji, X., Zhang, Y., Li, G., Sang, N., 2019. Gestational exposure to PM2.5 impairs vascularization of the placenta. Sci. Total Environ. 665, 153–161. https://doi.org/10.1016/j.scitotenv.2019.02.101. ⟨https://www.ncbi.nlm.nih.gov/pubmed/30772544⟩.

Zhao, M., Yang, Y., Bi, X., Yu, X., Jia, H., Fang, H., 2015. Acetylcholine attenuated TNF-alpha-induced apoptosis in H9c2 cells: role of calpain and the p38-MAPK pathway. Cell. Physiol. Biochem. 36 (5), 1877–1889. https://doi.org/10.1159/000430157. ⟨https://www.ncbi.nlm.nih.gov/pubmed/26183016⟩.

Zheng-Fischhofer, Q., Kibschull, M., Schnichels, M., Kretz, M., Petrasch-Parwez, E., Strotmann, J., et al., 2007. Characterization of connexin31.1-deficient mice reveals impaired placental development. Dev. Biol. 312 (1), 258–271. https://doi.org/10.1016/j.ydbio.2007.09.025. ⟨https://www.ncbi.nlm.nih.gov/pubmed/17961533⟩.

Zhu, N., Ji, X., Geng, X., Yue, H., Li, G., Sang, N., 2021. Maternal PM2.5 exposure and abnormal placental nutrient transport. Ecotoxicol. Environ. Saf. 207, 111281 https://doi.org/10.1016/j.ecoenv.2020.111281. ⟨https://www.ncbi.nlm.nih.gov/pubmed/32919195⟩.